Alignment of the CS_2 dimer embedded in helium droplets induced by a circularly polarized laser pulse

James D. Pickering, Benjamin Shepperson, Lars Christiansen, and Henrik Stapelfeldt*
Department of Chemistry, Aarhus University, Langelandsgade 140, 8000 Aarhus C, Denmark

(Received 2 January 2019; published 4 April 2019)

Dimers of carbon disulfide (CS_2) molecules embedded in helium nanodroplets are aligned using a moderately intense, 160-ps, nonresonant, circularly polarized laser pulse. It is shown that the intermolecular carbon-carbon (C-C) axis aligns along the axis perpendicular to the polarization plane of the alignment laser pulse. The degree of alignment, quantified by $\langle\cos^2\theta_{2D}\rangle$, is determined from the emission directions of recoiling CS_2^+ fragment ions, created when an intense 40-fs probe laser pulse doubly ionizes the dimers. Here, θ_{2D} is the projection of the angle between the C-C axis on the two-dimensional (2D) ion detector and the normal to the polarization plane. $\langle\cos^2\theta_{2D}\rangle$ is measured as a function of the alignment laser intensity and the results agree well with $\langle\cos^2\theta_{2D}\rangle$ calculated for gas-phase CS_2 dimers with a rotational temperature of 0.4 K.

DOI: 10.1103/PhysRevA.99.043403

I. INTRODUCTION

Recently, it has been shown that techniques used to align gas-phase samples of molecules based on the application of moderately intense laser pulses can be transferred to molecules inside helium nanodroplets [1–5]. This creates several opportunities. First, time-resolved imaging of molecular rotation, induced and probed by fs laser pulses, makes it possible to investigate how rotational quantum coherence, angular momentum, and energy are influenced by a dissipative environment [1,3,6–12]. Second, the 0.4-K temperature of He droplets is shared with the molecules residing inside the droplets [13]. Such a low temperature is highly beneficial for creating very strong alignment—not just for small molecules [4] but also for larger species [14], which can otherwise be difficult to effectively cool in the gas phase [15]. Third, the cold and dissipative environment of the He droplet provides unique opportunities for creating a variety of complexes of molecules and atoms [16,17]. Recently, it was shown that laser-induced alignment can also be applied efficiently to molecular complexes inside He droplets [18,19]. The high degrees of alignment made it possible to determine the structure of the molecular complexes by means of Coulomb explosion imaging induced by a high-intensity femtosecond laser pulse. Here we present a follow-up to our previous study of the CS_2 dimer [19], examining the alignment behavior of the dimer in more detail.

Alignment of molecules using linearly polarized laser pulses results in the confinement of the most polarizable axis of a molecule to the polarization axis of the aligning laser field and creates one-dimensional alignment [20]. This has been the most common use of laser-induced alignment in many prior studies. The most polarizable axis provides a "handle," which can be used to hold the molecule in advantageous spatial configurations using the alignment laser field [21]. However, it is also possible to align a molecule using a circularly (or elliptically) polarized laser field, which provides different handles and allows the molecule to be held in other spatial configurations than are possible with a linearly polarized field. Specifically, using a circularly polarized alignment field results in the alignment of the least polarizable molecular axis to the propagation axis of the alignment laser field [22]. This can be equivalently thought of as alignment of the most polarizable molecular plane to the polarization plane.

Our previous study of the CS_2 dimer solvated in He droplets [19] showed that it was possible to form, align, and image CS_2 dimers inside He droplets. Analysis of the recoil directions of CS_2^+ ions produced by Coulomb explosion of aligned CS_2 dimers showed that the structure of the CS_2 dimer in the He droplets was cross shaped with D_{2d} symmetry—which is also the structure in the gas phase [23,24]. Central to that study was the alignment of the CS_2 dimer (a symmetric top rotor) using a circularly polarized laser pulse. In the current work, we perform a detailed study of the intensity-dependent alignment of the CS_2 dimer in He droplets using a circularly polarized laser pulse. The alignment pulse duration of 160 ps places the alignment dynamics in the (quasi)adiabatic regime. To our knowledge very few studies so far have addressed alignment of symmetric top molecules with a circularly polarized alignment pulse, and only in the nonadiabatic limit using femtosecond alignment pulses [22,25].

II. BACKGROUND

A. Experimental methods

The experimental setup used to align and image the CS_2 dimers has already been described in detail elsewhere [4,19], with only relevant details reiterated here. The CS_2 molecules were embedded in He droplets consisting of around 8000 He atoms on average. The droplets are passed through a pickup cell containing CS_2 vapor, and the partial pressure of CS_2 was adjusted to a regime where substantial amounts of dimers (but minimal amounts of larger clusters) were formed. This is

*henriks@chem.au.dk

 ©2019 American Physical Society

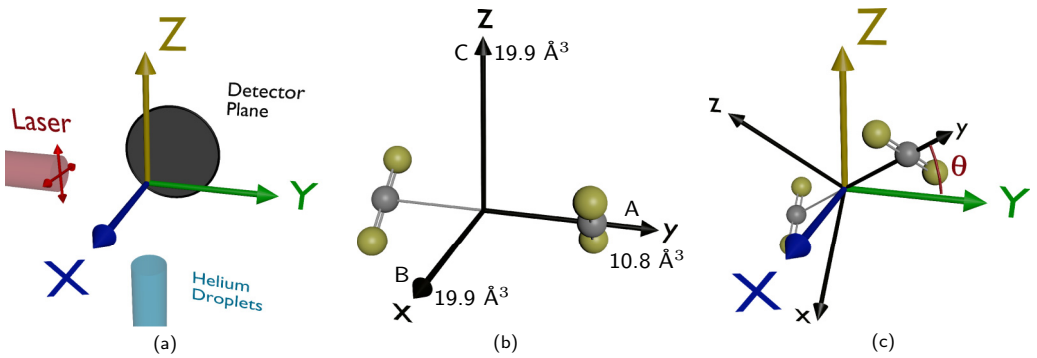

FIG. 1. (a) Sketch of the space-fixed (XYZ) coordinate system showing the propagation direction of the laser beams, the He droplet beam, and the detector. (b) Sketch of the molecular (xyz) coordinate system for the CS_2 dimer in its ground-state geometry. Polarizability elements of the dimer (in units of $\mathrm{\AA}^3$) are annotated onto each molecular axis, together with a label denoting which rotational constant (A, B, or C) is calculated around each axis (see text). (c) Sketch of the combined space-fixed (color) and molecular (black) coordinate systems, with the angle θ (between the y and the Y axes) shown in red.

defined as the dimer-doping condition—in line with previous work [19]. The doped droplet beam is then intersected at 90° by two focused laser beams from the same Ti-sapphire laser system. One beam consists of 160-ps [full width at half maximum (FWHM)] pulses ($\lambda_{\mathrm{center}} = 800$ nm) and is used to align the CS_2 dimers. The other beam consists of 40-fs (FWHM) pulses ($\lambda_{\mathrm{center}} = 800$ nm), and is used to Coulomb explode the dimers. The intensity of the probe pulses was 3×10^{14} W/cm^2, and the intensity of the alignment pulses was varied, up to a maximum value of 8×10^{11} W/cm^2. The temporal overlap of the two pulses was such that the probe pulse arrived at the peak of the alignment pulse. The nascent CS_2^+ ions were projected onto a 2D imaging detector using a velocity-map imaging spectrometer, and ion images were recorded.

Before discussing the details of laser-induced alignment, it is important to define the molecular (x, y, z) and space-fixed (X, Y, Z) coordinate systems. Figure 1(a) shows the space-fixed coordinate system. The laser beams propagate along the Y axis, such that the XZ plane is the polarization plane, and the He droplet beam propagates along the Z axis. Ions are accelerated along the X axis (the time-of-flight axis) towards a detector placed in the YZ plane. Figure 1(b) shows the structure of the CS_2 dimer in its ground-state geometry. The CS_2 dimer is a prolate symmetric top with a 90° angle between the two monomers, and in this case the symmetric top axis (the C-C axis) is placed along the y axis. The polarizability elements of the dimer are annotated on each molecular axis. In this case, the polarizability elements of the dimer were calculated simply by addition of the polarizability elements of the two monomers, each referenced to the molecular frame of the dimer. This method neglects any orbital interaction between the two monomers, but will not qualitatively change the polarizability elements of the dimer, so it is a reasonable first approximation to the true polarizability.

B. Alignment theory

The methodology and theory for alignment of molecules induced by strong laser fields has been described in several reviews [20,26,27]. Here we specifically consider the alignment of a symmetric top molecule using a circularly polarized laser pulse [22,25]. The interaction potential $\hat{V}(t)$ of a symmetric top molecule with a circularly polarized alignment field is given by [28]

$$\hat{V}(t) = -\tfrac{1}{4}E_0^2(t)[(\alpha_\perp - \alpha_\parallel)\cos^2(\theta) + \alpha_\parallel + \alpha_\perp], \quad (1)$$

where $E_0(t)$ is the electric-field envelope of the alignment laser field; $\alpha_\parallel$ is the polarizability of the molecule parallel to the symmetric top axis; $\alpha_\perp$ is the polarizability perpendicular to the symmetric top axis; and θ is the angle between the symmetric top axis and the normal to the polarization plane of the laser field. The alignment behavior is determined by the sign of the polarizability anisotropy, $\alpha_\parallel$-$\alpha_\perp$. If $\alpha_\parallel < \alpha_\perp$, which is typically the case for oblate symmetric top molecules like benzene (C_6H_6), ammonia (NH_3), or boron trifluoride (BF_3), the potential is at a minimum when $\theta = 0°$ and the interaction between the laser field and the molecule should lead to alignment of the symmetric top axis along the normal vector of the polarization plane, i.e., the propagation direction of the laser field. This has been illustrated for benzene molecules using nonadiabatic alignment induced by a 250-fs alignment pulse [22]. In contrast, if $\alpha_\perp < \alpha_\parallel$, which is typically the case for prolate symmetric top molecules like methyl iodide (CH_3I) or acetonitrile (CH_3CN), or for linear molecules, then the potential is at a minimum when $\theta = 90°$. In this case the symmetric top axis will be confined to (but randomly oriented in) the polarization plane.

For the CS_2 dimer $\alpha_\parallel < \alpha_\perp$ [Fig. 1(b)], although it is a prolate symmetric top. Thus, the expectation is that a circularly polarized alignment field will align the C-C axis (the y axis) along the propagation direction of the laser beam (the Y axis). A sketch of the combined space-fixed and molecule-fixed coordinate systems, and an illustration of the angle θ, is given in Fig. 1(c).

C. Computational methods

Recently, angulon theory [11,12] was used to rationalize that for the 160-ps alignment pulse used here, alignment of I_2, 1,4-diiodobenzene, and 1,4-dibromobenzene molecules inside He droplets is well described as alignment of gas-phase molecules with an effective rotational constant [4]. Qualitatively, this can be understood using the fact that the turn-on time of the alignment pulse is longer than the time scale

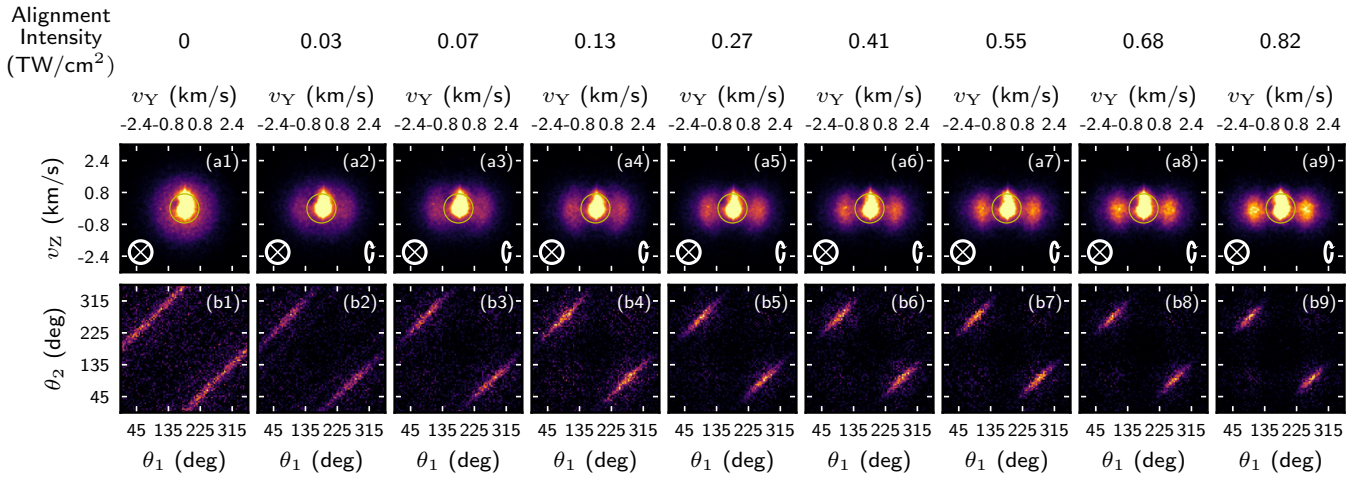

FIG. 2. (a1)–(a9) CS_2^+ ion images and (b1)–(b9) corresponding angular covariance maps calculated using ions outside the annotated yellow circles in row (a). The polarization state of the probe (alignment) laser is shown in the lower left (right) corner of each ion image. All data were recorded under the dimer-doping condition. The data in each column (1)–(9) were recorded at a different alignment intensity, annotated above each column.

of the He-He interactions and the He-molecule interactions. Therefore, a molecule and its solvation shell of He atoms has time to adjust as the laser field increases in strength. The CS_2 dimer is expected to behave similarly and thus we apply gas-phase alignment theory to calculate the degree of alignment of the dimer induced by the circularly polarized alignment pulse. In practice, the calculations were performed using an alignment calculator previously developed in our group [29]. This calculator solves the time-dependent rotational Schrödinger equation and returns the degree of alignment expressed as $\langle\cos^2\theta\rangle$ or $\langle\cos^2\theta_{2D}\rangle$. Here, θ_{2D} is the angle between the projection of the molecular C-C axis on the detector plane and the laser propagation axis. Calculation of $\langle\cos^2\theta_{2D}\rangle$ allows direct comparison of the calculations with the experimental data.

Strictly, the alignment calculator can only simulate alignment of linear or symmetric top molecules with $\alpha_\parallel > \alpha_\perp$ using linearly polarized alignment fields where the interaction potential is given by [30]

$$\hat{V}(t) = -\tfrac{1}{4}E_0^2(t)[(\alpha_\parallel - \alpha_\perp)\cos^2(\theta) + \alpha_\perp]. \qquad (2)$$

Comparison of Eqs. (1) and (2) shows that for a symmetric top molecule where $\alpha_\perp > \alpha_\parallel$ the angle-dependent part of the interaction potential induced by a circularly polarized field is the same as that for a linear molecule induced by a linearly polarized field. For the CS_2 dimer $\alpha_\perp > \alpha_\parallel$. This means that the alignment calculator can be used to calculate the degree of alignment of the CS_2 dimer induced by the circularly polarized field. We note that experimentally the peak intensity I_0, is determined. For a circularly polarized field the relation to the amplitude of the electric field E_0 is given by $I_0 = \varepsilon_0 c E_0^2$.

A detailed description of the alignment calculator can be found in Ref. [31], with only relevant parameters mentioned here. Calculations were performed at a variety of ensemble temperatures (see later), using the experimentally measured Gaussian focal spot sizes for both the alignment ($\omega_0 = 35\ \mu$m) and probe ($\omega_0 = 25\ \mu$m) beams. The degree of alignment was calculated using both the polarizability anisotropy determined by addition of the monomer polarizabilities ($\alpha_\parallel = 10.8$ Å^3, $\alpha_\perp = 19.9$ Å^3), and that calculated using density-functional theory (DFT—wB97XD/aug-pcseg-2) ($\alpha_\parallel = 12.0$ Å^3, $\alpha_\perp = 17.5$ Å^3) [19]. The effective rotational constant of a single CS_2 molecule inside He droplets has been calculated to be $0.3B_0$ [32], where B_0 is the gas-phase rotational constant ($0.109\ \text{cm}^{-1}$). A similar reduction is assumed for the CS_2 dimer, thus the rotational constants used in the calculation are $A = 0.0182\ \text{cm}^{-1}$, $B = C = 0.01281\ \text{cm}^{-1}$, where A is calculated around the molecular y axis, and B and C are calculated around the molecular x and z axes respectively. We note that in the (quasi)adiabatic limit defined by the 160-ps pulses the degree of alignment is very insensitive to the rotational constant, being essentially only determined by the polarizability anisotropy, rotational temperature of the molecular ensemble, and the intensity of the alignment pulse [33].

For completeness we address the question of why only alignment induced by a circularly polarized laser field and not by a linearly polarized laser field is studied here. The answer follows from Eq. (2), which shows that a linearly polarized field will confine θ to 90°. This means that the C-C axis will be perpendicular to and free to rotate around the alignment polarization axis. Such a situation implies less confinement of the spatial orientation of the dimer. As such, a circularly polarized alignment field is needed for creating one-dimensional (1D) alignment of a symmetric top molecule where $\alpha_\parallel < \alpha_\perp$, i.e., confining the symmetric top axis along the space-fixed axis defined by the propagation direction of the laser pulse. Similarly, a linearly polarized alignment field is needed to create 1D alignment of a symmetric top molecule (or a linear molecule) with $\alpha_\parallel > \alpha_\perp$.

III. RESULTS

Each column of Fig. 2 shows both a CS_2^+ ion image [row (a)], and corresponding angular covariance map [row (b)]. The angular covariance map [34] was calculated over all ion hits outside of the annotated yellow circle on the ion

image—this ensures that the covariance map is calculated using ion events arising from the Coulomb explosion of CS_2 dimers—as discussed in previous work [19]. The Coulomb explosion channel considered here is the one resulting from repulsion of two CS_2^+ ions created when each of the two CS_2 molecules in the dimer are singly ionized by the probe laser pulse. The ion signal inside the yellow circle arises from single ionization of CS_2 monomers. In all images, the probe pulse was linearly polarized along the X axis (shown in the lower left corner of each ion image), and the alignment pulse was circularly polarized in the XZ plane (shown in the lower right corner of each ion image). The alignment intensity used to record each image is shown above each column, and was incremented from 0 TW/cm^2 (column 1) to 0.82 TW/cm^2 (column 9). No ionization by the alignment pulse alone was observed, even at the highest intensity applied.

The ion signal outside the annotated yellow circle in images (a1)–(a9) of Fig. 2 moves from being isotropic (a1), to being strongly confined along the Y axis (a9) as the alignment intensity is increased from zero to its maximum value. This confinement is also reflected in the corresponding angular covariance maps (b1)–(b9), where the covariance signal changes from being a uniform line centered at $\theta_2 = \theta_1 + 180^\circ$ or at $\theta_2 = \theta_1 - 180^\circ$ [panel (b1)], to a confined island centered at $(90^\circ, 270^\circ)$, and the equivalent island at $(270^\circ, 90^\circ)$ [panel (b9)]. It is clear from both the ion images and covariance maps that the degree of alignment increases as the alignment intensity is increased from column (1) to column (9), and that the degree of alignment appears to saturate at around column (5)—increasing the intensity beyond this level does not seem to dramatically increase the observed degree of alignment. This can be quantified by calculating $\langle \cos^2 \theta_{2D} \rangle$, but it is useful to first consider the explosion process in He droplets in more detail.

Prior studies of aligned molecules in He droplets have shown that the recoil trajectories of the nascent ion fragments following Coulomb explosion are distorted due to scattering off the He atoms as they exit the droplet. This results in nonaxial recoil (NAR), where the recoil trajectories of the nascent ions no longer directly reflect the alignment of the molecular axis they recoiled from. In studies of laser-induced alignment inside He droplets, calculating $\langle \cos^2 \theta_{2D} \rangle$ from an ion image without correcting for NAR leads to an underestimate of the true degree of alignment. However, the effect of the NAR can be determined from the correlation between the fragment ions (here the CS_2^+ ions) using covariance analysis, and deconvoluted from the fragment angular distributions, allowing the true degree of alignment to be obtained [35]. This has been implemented in the study of aligned molecules in He droplets previously [4].

Figure 3(a) shows the experimentally measured (crosses) and the simulated (circular markers and dashed line) degree of alignment ($\langle \cos^2 \theta_{2D} \rangle$) of the CS_2 dimer as a function of the alignment pulse intensity (the highest J state included in the calculation was $J = 50$). The grey crosses (lower crosses) represent the degree of alignment determined from the CS_2^+ ion images without any correction for NAR, whereas the black crosses (upper crosses) show the same measurements, corrected for NAR. The blue simulated trace (lower trace - dotted line) was calculated using a polarizability anisotropy calculated using DFT assuming an intermonomer separation of 3.5 Å (such that $\Delta\alpha = 5.5$ Å^3), whereas the green trace (upper trace, dashed line) was calculated using a polarizability anisotropy calculated by addition of the polarizability tensors of the two CS_2 monomers (such that $\Delta\alpha = 9.1$ Å^3). Figure 3(b) again shows the experimentally measured degree of alignment, corrected for NAR (crosses), together with the simulated degree of alignment calculated at a variety of different ensemble temperatures from 0.1 K [upper line (dashed)] to 1.0 K [lower

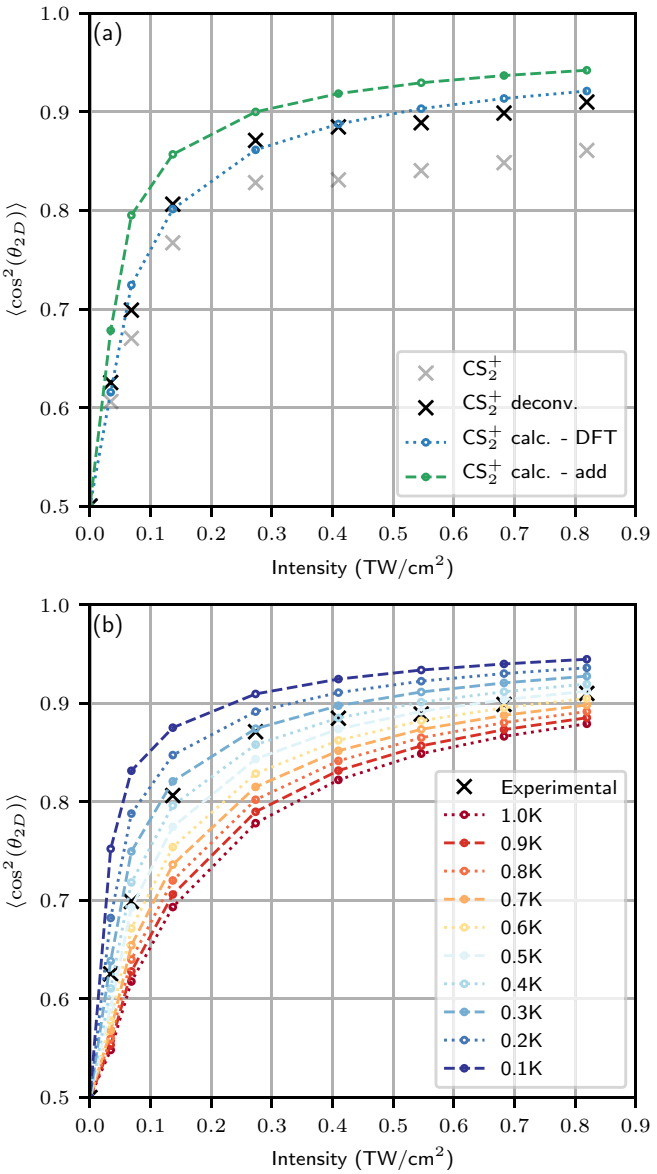

FIG. 3. Experimental (crosses) and simulated (circles and dashed or dotted lines) degree of alignment of the CS_2 dimer as a function of alignment intensity. The alignment was induced adiabatically using a circularly polarized laser pulse. Panel (a) shows a comparison of the experimental degree of alignment with the simulated degree of alignment calculated at 0.4 K, using two different polarizability anisotropies (see text). Panel (b) shows a comparison of the experimental degree of alignment with the simulated degree of alignment calculated at a variety of different ensemble temperatures (see text).

line (dotted)] in steps of 0.1 K. The line style alternates from dashed to dotted at each step of 0.1 K. For all the different ensemble temperatures, the polarizability anisotropy was chosen to be that which was calculated using DFT.

IV. DISCUSSION

Examining Fig. 3(a), several observations can be made. First, it is clear that the observed degree of alignment rapidly increases as the alignment intensity is raised, before levelling out at higher intensities. Second, the deconvoluted data [black (upper) crosses] shows a higher degree of alignment than the data obtained directly from the ion images [grey (lower) crosses], as is expected due to the NAR in He droplets. Accordingly, the deconvoluted data are a better match to the simulated traces than the nondeconvoluted data. Additionally, the simulated trace that best matches the experimental data is the one employing a polarizability anistropy calculated by DFT methods, rather than that calculated via addition of the polarizability tensors of the two monomers.

The polarizability anisotropy calculated by DFT is less than the anisotropy calculated via addition of the polarizability tensors of the two monomers. This implies that there is some electronic (orbital) interaction between the two CS_2 units in the dimer, as the simple addition of polarizability elements neglects this. The electronic interaction lowers the overall polarizability anisotropy as the electron density in the region between the two CS_2 molecules is increased. This suggests that the interaction between the two CS_2 monomers has some orbital character—in addition to the expected (nonorbital) van der Waals interaction [36]. The sensitivity to the polarizability anisotropy in this way illustrates the potential utility of laser-induced alignment as a diagnostic tool for studying noncovalent interactions and that it may be possible to gain some deeper insight into the electronic structure of such complexes with further study.

Turning to Fig. 3(b), it appears that the experimental data correspond well to the simulated data using an ensemble temperature of between 0.3 and 0.5 K. This agreement implies that the alignment of the CS_2 dimers in the He droplets is consistent with alignment of a 0.4-K ensemble of gas-phase CS_2 dimers. This is completely in line with the expected temperature of the dimers inside the He droplets [13].

V. CONCLUSION

We have shown that the C-C axis of CS_2 dimers embedded in He droplets can be tightly confined along the propagation direction of a circularly polarized 160-ps laser pulse. The degree of this one-dimensional alignment was measured as a function of the intensity of the alignment pulse by Coulomb explosion imaging with an intense 40-fs probe pulse. It was found that the measured degree of alignment, $\langle\cos^2\theta_{2D}\rangle$, as a function of intensity, matched well with $\langle\cos^2\theta_{2D}\rangle$ calculated for a sample of CS_2 dimers with an adjusted rotational constant and a temperature of 0.4 K. As such, our results corroborate and generalize recent findings on I_2 molecules in He droplets where the experimentally recorded degree of one-dimensional alignment, induced by a linearly polarized laser field, also agreed well with calculations of $\langle\cos^2\theta_{2D}\rangle$ for a 0.4-K ensemble of I_2 molecules with an adjusted rotational constant. Since molecules and complexes of molecules embedded in He droplets should, in general, thermalize to the 0.4-K environment we believe that the high degree of alignment enabled by the low temperature can be obtained for a wide variety of species. This will prove advantageous for applications that benefit from such rigorous control of the molecular frame, including diffractive imaging with (soft) x rays [37–40], Coulomb explosion imaging [19], and electron diffraction [41,42].

[1] D. Pentlehner, J. H. Nielsen, A. Slenczka, K. Mølmer, and H. Stapelfeldt, Impulsive Laser Induced Alignment of Molecules Dissolved in Helium Nanodroplets, Phys. Rev. Lett. **110**, 093002 (2013).

[2] D. Pentlehner, J. H. Nielsen, L. Christiansen, A. Slenczka, and H. Stapelfeldt, Laser-induced adiabatic alignment of molecules dissolved in helium nanodroplets, Phys. Rev. A **87**, 063401 (2013).

[3] B. Shepperson, A. A. Søndergaard, L. Christiansen, J. Kaczmarczyk, R. E. Zillich, M. Lemeshko, and H. Stapelfeldt, Laser-Induced Rotation of Iodine Molecules in Helium Nanodroplets: Revivals and Breaking Free, Phys. Rev. Lett. **118**, 203203 (2017).

[4] B. Shepperson, A. S. Chatterley, A. A. Søndergaard, L. Christiansen, M. Lemeshko, and H. Stapelfeldt, Strongly aligned molecules inside helium droplets in the near-adiabatic regime, J. Chem. Phys. **147**, 013946 (2017).

[5] A. S. Chatterley, B. Shepperson, and H. Stapelfeldt, Three-Dimensional Molecular Alignment Inside Helium Nanodroplets, Phys. Rev. Lett. **119**, 073202 (2017).

[6] B. Shepperson, A. S. Chatterley, L. Christiansen, A. A. Søndergaard, and H. Stapelfeldt, Observation of rotational revivals for iodine molecules in helium droplets using a near-adiabatic laser pulse, Phys. Rev. A **97**, 013427 (2018).

[7] S. Ramakrishna and T. Seideman, Intense Laser Alignment in Dissipative Media as a Route to Solvent Dynamics, Phys. Rev. Lett. **95**, 113001 (2005).

[8] T. Vieillard, F. Chaussard, D. Sugny, B. Lavorel, and O. Faucher, Field-free molecular alignment of CO_2 mixtures in presence of collisional relaxation, J. Raman Spectrosc. **39**, 694 (2008).

[9] J. Lindgren and T. Kiljunen, Excitation of rotons in parahydrogen crystals: The laser-induced-molecular-alignment mechanism, Phys. Rev. A **88**, 043420 (2013).

[10] B. A. Stickler, B. Schrinski, and K. Hornberger, Rotational Friction and Diffusion of Quantum Rotors, Phys. Rev. Lett. **121**, 040401 (2018).

[11] R. Schmidt and M. Lemeshko, Rotation of Quantum Impurities in the Presence of a Many-Body Environment, Phys. Rev. Lett. **114**, 203001 (2015).

[12] M. Lemeshko, Quasiparticle Approach to Molecules Interacting with Quantum Solvents, Phys. Rev. Lett. **118**, 095301 (2017).

[13] J. P. Toennies and A. F. Vilesov, Superfluid helium droplets: A uniquely cold nanomatrix for molecules and molecular complexes, Angew. Chem. Int. Ed. **43**, 2622 (2004).
[14] A. S. Chatterley, C. Schouder, L. Christiansen, B. Shepperson, M. H. Rasmussen, and H. Stapelfeldt, Long-lasting field-free alignment of large molecules inside helium nanodroplets, Nat. Commun. **10**, 133 (2019).
[15] G. Meijer, M. S. Vries, H. E. Hunziker, and H. R. Wendt, Laser desorption jet-cooling of organic molecules, Appl. Phys. B **51**, 395 (1990).
[16] M. Y. Choi, G. E. Douberly, T. M. Falconer, W. K. Lewis, C. M. Lindsay, J. M. Merritt, P. L. Stiles, and R. E. Miller, Infrared spectroscopy of helium nanodroplets: novel methods for physics and chemistry, Int. Rev. Phys. Chem. **25**, 15 (2006).
[17] S. Yang and A. M. Ellis, Helium droplets: A chemistry perspective, Chem. Soc. Rev. **42**, 472 (2012).
[18] J. D. Pickering, B. Shepperson, L. Christiansen, and H. Stapelfeldt, Femtosecond laser-induced coulomb explosion imaging of aligned OCS oligomers inside helium nanodroplets, J. Chem. Phys. **149**, 154306 (2018).
[19] J. D. Pickering, B. Shepperson, B. A. K. Hübschmann, F. Thorning, and H. Stapelfeldt, Alignment and Imaging of the CS_2 Dimer Inside Helium Nanodroplets, Phys. Rev. Lett. **120**, 113202 (2018).
[20] H. Stapelfeldt and T. Seideman, Colloquium: Aligning molecules with strong laser pulses, Rev. Mod. Phys. **75**, 543 (2003).
[21] M. Burt, K. Amini, J. W. L. Lee, L. Christiansen, R. R. Johansen, Y. Kobayashi, J. D. Pickering, C. Vallance, M. Brouard, and H. Stapelfeldt, Communication: Gas-phase structural isomer identification by coulomb explosion of aligned molecules, J. Chem. Phys. **148**, 091102 (2018).
[22] C. T. L. Smeenk and P. B. Corkum, Molecular alignment using circularly polarized laser pulses, J. Phys. B: At. Mol. Opt. Phys. **46**, 201001 (2013).
[23] N. Moazzen-Ahmadi and A. R. W. McKellar, Spectroscopy of dimers, trimers and larger clusters of linear molecules, Int. Rev. Phys. Chem. **32**, 611 (2013).
[24] M. Rezaei, J. Norooz Oliaee, N. Moazzen-Ahmadi, and A. R. W. McKellar, Spectroscopic observation and structure of CS_2 dimer, J. Chem. Phys. **134**, 144306 (2011).
[25] C. T. L. Smeenk, L. Arissian, A. V. Sokolov, M. Spanner, K. F. Lee, A. Staudte, D. M. Villeneuve, and P. B. Corkum, Alignment Dependent Enhancement of the Photoelectron Cutoff for Multiphoton Ionization of Molecules, Phys. Rev. Lett. **112**, 253001 (2014).
[26] T. Seideman and E. Hamilton, Nonadiabatic alignment by intense pulses. concepts, theory, and directions, Adv. At. Mol. Opt. Phys. **52**, 289 (2005).
[27] S. Fleischer, Y. Khodorkovsky, E. Gershnabel, Y. Prior, and I. S. Averbukh, Molecular alignment induced by ultrashort laser pulses and its impact on molecular motion, Isr. J. Chem. **52**, 414 (2012).
[28] J. J. Larsen, Laser Induced Alignment of Neutral Molecules, Ph.D. thesis, Aarhus University, 2000.
[29] A. A. Søndergaard, B. Shepperson, and H. Stapelfeldt, Nonadiabatic laser-induced alignment of molecules: Reconstructing $\langle\cos^2\theta\rangle$ directly from $\langle\cos^2\theta_{2D}\rangle$ by Fourier analysis, J. Chem. Phys. **147**, 013905 (2017).
[30] B. Friedrich and D. Herschbach, Alignment and Trapping of Molecules in Intense Laser Fields, Phys. Rev. Lett. **74**, 4623 (1995).
[31] A. A. Søndergaard, Understanding Laser-Induced Alignment and Rotation of Molecules Embedded in Helium Nanodroplets, Ph.D. thesis, Aarhus University, 2016.
[32] R. Zillich (private communication).
[33] T. Seideman, On the dynamics of rotationally broad, spatially aligned wave packets, J. Chem. Phys. **115**, 5965 (2001).
[34] J. L. Hansen, J. H. Nielsen, C. B. Madsen, A. T. Lindhardt, M. P Johansson, T. Skrydstrup, L. B. Madsen, and H. Stapelfeldt, Control and femtosecond time-resolved imaging of torsion in a chiral molecule, J. Chem. Phys. **136**, 204310 (2012).
[35] L. Christensen, L. Christiansen, B. Shepperson, and H. Stapelfeldt, Deconvoluting nonaxial recoil in Coulomb explosion measurements of molecular axis alignment, Phys. Rev. A **94**, 023410 (2016).
[36] P. Hobza and K. Dethlefs-Müller, *Non-Covalent Interactions, Theory and Experiment* (RSC Publishing, Cambridge, 2010).
[37] J. Küpper, S. Stern, L. Holmegaard, F. Filsinger, A. Rouzée, A. Rudenko, P. Johnsson, A. V. Martin, M. Adolph, A. Aquila, S. Bajt, A. Barty, C. Bostedt, J. Bozek, C. Caleman, R. Coffee, N. Coppola, T. Delmas, S. Epp, B. Erk *et al.*, X-Ray Diffraction from Isolated and Strongly Aligned Gas-Phase Molecules with a Free-Electron Laser, Phys. Rev. Lett. **112**, 083002 (2014).
[38] L. F. Gomez, K. R. Ferguson, J. P. Cryan, C. Bacellar, R. M. P. Tanyag, C. Jones, S. Schorb, D. Anielski, A. Belkacem, C. Bernando, R. Boll, J. Bozek, S. Carron, G. Chen, T. Delmas, L. Englert, S. W. Epp, B. Erk, L. Foucar, R. Hartmann *et al.*, Shapes and vorticities of superfluid helium nanodroplets, Science **345**, 906 (2014).
[39] R. M. P. Tanyag, C. Bernando, C. F. Jones, C. Bacellar, K. R. Ferguson, D. Anielski, R. Boll, S. Carron, J. P. Cryan, L. Englert, S. W. Epp, B. Erk, L. Foucar, L. F. Gomez, R. Hartmann, D. M. Neumark, D. Rolles, B. Rudek, A. Rudenko, K. R. Siefermann *et al.*, Communication: X-ray coherent diffractive imaging by immersion in nanodroplets, Struct. Dyn. **2**, 051102 (2015).
[40] D. Rupp, N. Monserud, B. Langbehn, M. Sauppe, J. Zimmermann, Y. Ovcharenko, T. Möller, F. Frassetto, L. Poletto, A. Trabattoni, F. Calegari, M. Nisoli, K. Sander, C. Peltz, M. J. Vrakking, T. Fennel, and A. Rouzée, Coherent diffractive imaging of single helium nanodroplets with a high harmonic generation source, Nat. Commun. **8**, 493 (2017).
[41] Y. He, J. Zhang, L. Lei, and W. Kong, Self-assembly of iodine in superfluid helium droplets: Halogen bonds and nanocrystals, Angew. Chem. **129**, 3595 (2017).
[42] J. Zhang, Y. He, W. M. Freund, and W. Kong, Electron diffraction of superfluid helium droplets, J. Phys. Chem. Lett. **5**, 1801 (2014).